Rhodium(I) and Iridium(I) Complexes Containing β-Diketonate or Pyrazole Ligands. Liquid Crystal and Nonlinear Optical Properties

Joaquín Barberá,[†] Anabel Elduque,[‡] Raquel Giménez,[†] Fernando J. Lahoz,[‡] José A. López,[‡] Luis A. Oro,*[,‡] José Luis Serrano,*[,†] Belén Villacampa,[§] and Julio Villalba[§]

Departamento de Química Orgánica, Departamento de Química Inorgánica, and Departamento de Física de la Materia Condensada, Instituto de Ciencia de Materiales de Aragón, Universidad de Zaragoza-Consejo Superior de Investigaciones Científicas, 50009 Zaragoza, Spain

Received December 8, 1998

Square-planar rhodium or iridium "*n*-decyloxy-β-diketonate" complexes of the general formula [M(β-diketonate)-$(CO)_2$] (M = Rh (**1**−**3**) or Ir (**4**−**6**)) and pyrazole−rhodium derivatives of the type [RhCl$(CO)_2$(pyrazole)] (**7**−**9**) have been prepared and their liquid-crystalline properties studied. Compounds **1** and **4** show monotropic smectic A phases, and complex **7** shows a monotropic nematic phase. The behavior of the melting points seems to be related to the X group directly bonded at the 3-position of the β-diketonate ligand (**1**−**6**) or at the 4-position of the pyrazole ring (**7**−**9**). When X = OOC higher melting points are obtained. Two different polymorphs, red (M = Rh) or blue (M = Ir) and yellow (M = Rh, Ir), have been obtained for complexes **1**, **4**, and **6**. The yellow form for compound **4** ($C_{31}H_{35}IrO_9 \cdot CH_3OH$, monoclinic system, space group $P2_1/c$ (No. 14) with $a = 26.991(6)$ Å, $b = 4.0093(8)$ Å, $c = 31.169(6)$ Å, $\beta = 104.950(13)°$, and $Z = 4$) has also been characterized by an X-ray single-crystal diffraction experiment in order to explain the influence of the packing arrangement in the formation of different polymorphs. Additionally, measurements of the first-order optical hyperpolarizability (β) of the rhodium compounds and some of the precursor ligands using the EFISH technique have also been performed.

Introduction

In pursuance of our research on liquid crystals based on β-diketone, pyrazole, and isoxazole derivatives,[1] we became interested in the design of new structures exhibiting improved properties by the incorporation of metal atoms into organic molecules.[2] Specific properties such as color, paramagnetism, electric conductivity, etc., can be obtained more easily in metal−organic complexes than in purely organic compounds.[3] Furthermore, other molecular properties such as polarizability or hyperpolarizability can be enhanced by the presence of metals.[3]

Few examples of calamitic (rodlike) liquid crystals containing rhodium or iridium have been described in the literature,[3c,4−6] and they have a *cis*-[MCl$(CO)_2$L] structure (M = Rh or Ir; L = nitrogen-donor promesogenic ligand).[5] Taking advantage of the mesogenicity of certain β-diketone and pyrazole ligands previously reported by our group (Scheme 1, ligands HL_1−HL_3, HL'_1−HL'_3)[1c] and their ability to coordinate metal atoms, we decided to prepare and investigate the liquid crystal properties of new rhodium and iridium complexes containing these rodlike β-diketonate and pyrazole ligands. The resulting compounds can exhibit conjugated structures in which the metal environments, [M$(CO)_2$] or [RhCl$(CO)_2$], act as a terminal polar group and the decyloxy group, at the other end of the molecule, could play the role of an electron-donor group. These compounds therefore fulfill a priori the requirements for second harmonic generation and thus are potentially interesting for nonlinear optic studies.

We report new rhodium− and iridium−β-diketonate complexes as well as the first organometallic pyrazole derivative presenting a liquid crystal behavior. Part of this work has been preliminarily communicated.[7] We have also performed measurements of the first-order optical hyperpolarizability (β) of the

[†] Departamento de Química Orgánica.
[‡] Departamento de Química Inorgánica.
[§] Departamento de Física de la Materia Condensada.

(1) (a) Barberá, J.; Cativiela, C.; Serrano, J. L.; Zurbano, M. M. *Liq. Cryst.* **1992**, *11*, 887. (b) Barberá, J.; Giménez, R.; Serrano, J. L. *Adv. Mater.* **1994**, *6*, 470. (c) Cativiela, C.; Serrano, J. L.; Zurbano, M. M. *J. Org. Chem.* **1995**, *60*, 3074. (d) Iglesias, R.; Serrano, J. L.; Sierra, T. *Liq. Cryst.* **1997**, *22*, 37.

(2) (a) Barberá, J.; Cativiela, C.; Serrano, J. L.; Zurbano, M. M. *Adv. Mater.* **1991**, *3*, 602. (b) Atencio, R.; Barberá, J.; Cativiela, C.; Lahoz, F. J.; Serrano, J. L.; Zurbano, M. M. *J. Am. Chem. Soc.* **1994**, *116*, 11558. (c) Barberá, J.; Elduque, A.; Giménez, R.; Oro, L. A.; Serrano, J. L. *Angew. Chem., Int. Ed. Engl.* **1996**, *35*, 2832. (d) Barberá, J.; Elduque, A.; Giménez, R.; Lahoz, F. J.; López, J. A.; Oro, L. A.; Serrano, J. L. *Inorg. Chem.* **1998**, *37*, 2961.

(3) (a) Ros, M. B. In *Metallomesogens. Synthesis, Properties and Applications*; Serrano, J. L., Ed.; VCH: Weinheim, Germany, 1996, Chapter 11. (b) Bruce, D. W. *J. Chem. Soc., Dalton Trans.* **1993**, 2984. (c) Espinet, P.; Esteruelas, M. A.; Oro, L. A.; Serrano, J. L.; Sola, E. *Coord. Chem. Rev.* **1992**, *117*, 215.

(4) Serrano, J. L.; Sierra, T. In *Metallomesogens. Synthesis, Properties and Applications*; Serrano, J. L., Ed.; VCH: Weinheim, Germany, 1996; Chapter 3.

(5) (a) Bruce, D. W.; Lalinde, E.; Styring, P.; Dunmur, D. A.; Maitlis, P. M. *J. Chem. Soc., Chem. Commun.* **1986**, 581. (b) Esteruelas, M. A.; Sola, E.; Oro, L. A.; Ros, M. B.; Serrano, J. L. *J. Chem. Soc., Chem. Commun.* **1989**, 55. (c) Esteruelas; M. A.; Sola, E.; Oro, L. A.; Ros, M. B.; Marcos, M.; Serrano, J. L. *J. Organomet. Chem.* **1990**, *387*, 103. (d) Bruce, D. W.; Dunmur, D. A.; Esteruelas, M. A.; Hunt, S. E.; Le Lagadec, R.; Maitlis, P. M.; Marsden, J. R.; Sola, E.; Stacey, J. M. *J. Mater. Chem.* **1991**, *1*, 251. (e) Adams, H.; Bailey, N. A.; Bruce, D. W.; Hudson, S. A.; Marsden, J. R. *Liq. Cryst.* **1994**, *16*, 643.

(6) (a) Berdagué, P.; Courtieu, J.; Maitlis, P. M. *J. Chem. Soc., Chem. Commun.* **1994**, 1313. (b) Bruce, D. W.; Hall, M. D. *Mol. Cryst. Liq. Cryst.* **1994**, *250*, 373.

(7) Giménez, R.; Barberá, J.; Serrano, J. L.; Oro, L. A.; Elduque, A. *International Symposium on Metallomesogens*, 4th, Università della Calabria, Cetraro, Italy; 1995.

10.1021/ic9814017 CCC: $18.00
Published on Web 05/29/1999

Scheme 1

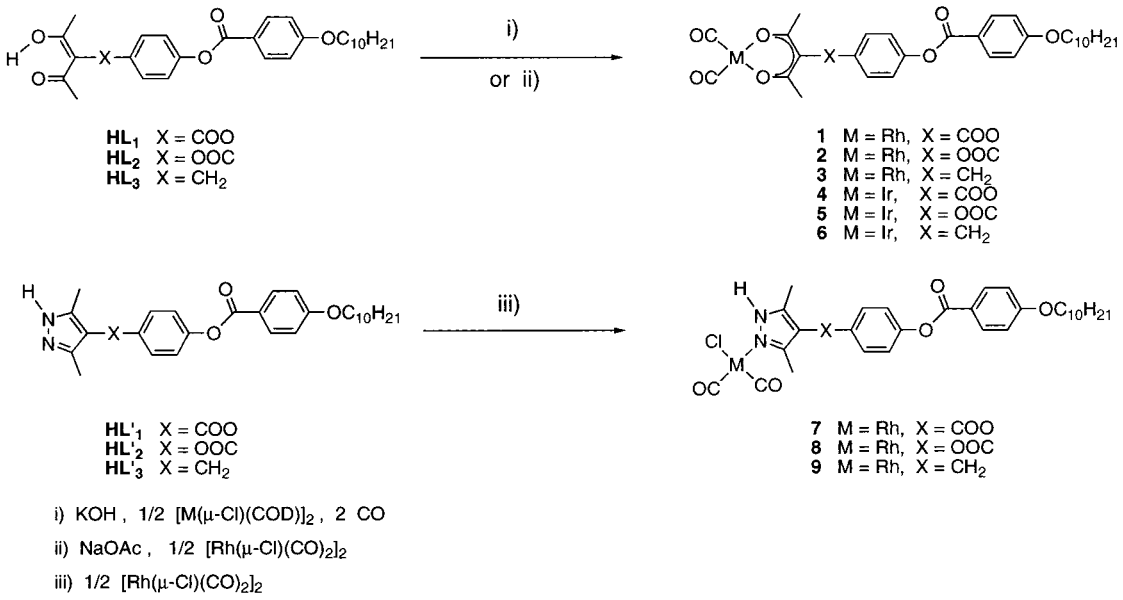

rhodium complexes and some of the precursor ligands using the EFISH technique.[8] The aim of this study is to evaluate the effect of the presence of the metal on the nonlinear response of the molecule as well as to check the influence of the different groups X (see Scheme 1) in the conjugation path.

Results and Discussion

Preparation of Rhodium and Iridium β-Diketonate Complexes. Complexes of general formula [M(β-diketonate)$(CO)_2$] (M = Rh, Ir) (**1**−**6**), have been prepared in accordance with Scheme 1, i. Compounds **1**−**3** have also been obtained by direct reaction of sodium diketonate salts and the tetracarbonyl rhodium complex $[Rh_2(\mu\text{-}Cl)_2(CO)_4]$ (Scheme 1, ii).

The ^{1}H NMR spectra of complexes **1**−**6** in $CDCl_3$ solutions confirm the coordination of the β-diketonate groups to the metal centers.

Complexes **2** and **5** are yellow, while compound **3** was isolated as a red solid. However, two different polymorphs were obtained for complexes **1**, **4**, and **6** depending on the solid formation conditions: a red (M = Rh) or dark blue (M = Ir) polymorph and the other yellow (M = Rh, Ir). The more colored forms (red or blue), obtained at higher temperatures, show, in the solid state, complex IR spectra probably due to metal stacking as a consequence of the d_{z^2} orbital interactions, as previously observed for related complexes.[9] The yellow color of the second polymorph, together with a simpler IR spectrum (see Table 1) suggest a packing arrangement without intermetallic interactions,[10] as has been observed for complex **4** by an X-ray crystallographic study (see below). The red (M = Rh) or blue (M = Ir) solid polymorphs transform to the yellow form, in solution. The existence of two polymorphic forms for related complexes has previously been reported.[10d−e]

Table 1. Thermal Behavior (Transition Temperatures and Enthalpies, Determined by OM and DSC) and IR $\nu_{C\equiv O}$ Absorptions (Nujol Suspension) of Complexes **1**, **4**, and **6**[a]

compd	OM−DSC [°C (KJ mol^{-1})]	IR $\nu_{C\equiv O}$ (cm^{-1})
1 (yellow form)	C, 80 (6.1); C′, 101 (48.5); I	2088, 2027
1 (red form)	C′, 100 (51.5); I	2081, 2027^{sh}, 2005, 1978^{sh}
4 (yellow form)	C, 78 (19.4); C′, 128 (39.9); I	2079, 1997^{br}
4 (blue form)	C′, 123 (27.9); I	2067, 2022^{br}, 1983
6 (yellow form)	C, 112 C′, 118 I	2044, 1988, 1977
6 (blue form)	C′, 116 (28.9); I	2054, 2006^{br}, 1979, 1970

[a] C, C′, crystal phases; I, isotropic liquid; sh, shoulder; br, broad signal.

We have also studied the thermochromism of complexes **1**, **4**, and **6** by optical microscopy. Heating the yellow-colored solids causes them to change to the dark colored forms (red M = Rh or blue M = Ir). Finally, yellow isotropic liquids were obtained. In parallel, a thermal study has been performed by differential scanning calorimetry (DSC), and the results are shown in Table 1. The yellow samples exhibit one crystal−crystal transition (C−C′), corresponding to the transformation to the dark polymorphs observed under the optical microscope, and a crystal-liquid (C′−I) transition. The dark forms only show a crystal−isotropic liquid transition.

Preparation of Rhodium Pyrazole Complexes. Yellow complexes of general formula *cis*-[RhCl$(CO)_2$(pyrazole)] (pyrazole = HL′$_1$ (**7**), HL′$_2$ (**8**), HL′$_3$ (**9**)) were prepared by reaction of $[Rh_2(\mu\text{-}Cl)_2(CO)_4]$ with the corresponding pyrazole ligand (Scheme 1, iii). These complexes were characterized by analytical and spectroscopic methods. In particular, the ^{1}H NMR spectra of these compounds show a singlet at δ = 11.5 ppm corresponding to the NH proton and two singlets in the range 2.15−2.57 ppm, indicating the inequivalence of the methyl groups of the pyrazole ligands.

Mesomorphic Properties. Complexes **1**−**9** have been studied by optical microscopy with polarized light and a heating−cooling stage and by DSC. The results obtained are summarized in Table 2.

(8) (a) Levine, B. F.; Bethea, C. G. *J. Chem. Phys*. **1975**, *63*, 2666. (b) Oudar, J. L. *Chem. Phys*. **1977**, *67*, 446.
(9) Aullón, G.; Alvarez, S. *Chem. Eur. J*. **1997**, *3*, 655, and references cited therein.
(10) (a) Gordon, G. C.; Dehaven, P. W.; Weiss, M. C.; Goedken, V. L. *J. Am. Chem. Soc*. **1978**, *100*, 1003. (b) Elduque, A.; Finestra, C.; López, J. A.; Lahoz, F. J.; Merchán, F.; Oro, L. A.; Pinillos, M. T. *Inorg. Chem*. **1998**, *37*, 824. (c) Kolel-Veetil, M. K.; Rheingold, A. L.; Ahmed, K. J. *Organometallics* **1993**, *12*, 3439. (d) Pannetier, G.; Bonnaire, R.; Fougeroux, P.; Davignon, L.; Platzer, N. *J. Organomet. Chem*. **1973**, *54*, 313. (e) Davignon, L.; Manoli, J. M.; Dereigne, A. *J. Less-Common Met*. **1976**, *44*, 201.

Table 2. Optical, Thermal, and Thermodynamical Properties of Ligands HL_1−HL_3 and Their Complexes **1**−**6** and of Ligands HL'_1−HL'_3 and Their Complexes **7**−**9**

compd	X	transition	T (°C)	ΔH (kJ mol^{-1})
HL_1	COO	C_1-C_2	27.7	3.8
		C_2-I	65.9	37.5
		$I-N^a$	50.7	−0.4
		$N-S_A{}^a$	45.2	−0.4
HL_2	OOC	C_1-C_2	25.1	1.0
		C_2-C_3	46.4	18.3
		C_3-I	79.4	15.6
		$I-N^a$	27.5	−0.9
		$N-S_A{}^a$	24.9	−0.6
HL_3	CH_2	C_1-I	49.8	42.7[b]
		C_2-I	55.8	
1	COO	C_1-C_2	80.2	6.1
		C_2-I	100.8	48.5
		$I-S_A{}^a$	93.8	−3.7
2	OOC	C−I	144.6	36.9
3	CH_2	C−I	111.3	32.9
4	COO	C_1-C_2	78.0	19.4
		C_2-I	127.6	39.9
		$I-S_A{}^a$	96.0	*c*
5	OOC	C−I	128.1	18.2
6	CH_2	C−I	116.1	28.9
HL_1'	COO	C_1-C_2	68.6	2.3
		C_2-C_3	94.3	4.4
		C_3-I	156.0	31.6
		$I-N^a$	146[d]	−
HL_2'	OOC	C−I	125.3	21.4
		$I-N^a$	78.9	−0.9
HL_3'	CH_2	C_1-C_2	49.7	0.6
		C_2-C_3	75.8	2.2
		C_3-C_4	101.3	1.1
		C_4-I	136.7	25.0
7	COO	C−I	139.7	26.9
		$I-N^a$	123.5	−0.6
8	OOC	C−I	126.2	23.4
9	CH_2	C_1-C_2	73.6	29.1
		C_2-I	87.4	21.6

[a] Monotropic transition. [b] Includes both transitions. [c] No enthalpy value could be obtained due to partial overlapping with the crystallization peak. [d] Optical microscopy data.

Diketonate Derivatives (1−6) (Table 2). Complexes **1** and **4** show a monotropic smectic A phase. Under the optical microscope with polarized light the textures are fan-shaped with homeotropic regions. Figure 1a corresponds to the mesophase of **1**. The thermograms show that, on cooling the isotropic liquid at 10 °C min^{-1}, the mesophase of compound **1** appears at 93.8° and remains over 20 °C. In the case of the iridium complex **4** the mesophase appearance and the crystallization are almost simultaneous, showing a DSC thermogram with these two transitions partially overlapped. This fact prevented us from calculating the enthalpy for the isotropic liquid−mesophase transition. Complexes **2**, **3**, **5**, and **6** did not show liquid crystal properties. Melting points are, in general, between 111 and 145 °C.

The β-diketone ligands HL_1 (X = COO) and HL_2 (X = OOC) show monotropic nematic and smectic A mesophases[1c] characterized by their typical textures (Schlieren and fan-shaped, respectively), and their melting points are always lower than those of the related complexes. [These data present some disagreement with those reported in a recent publication where a nonmesogenic behavior for the β-diketonate ligand HL_2 (X = OOC) is described.[11]] Comparing the complexes with their respective ligands, the group $[M(CO)_2]$ makes the molecule longer without varying significantly the molecular width, and this fact should benefit, in a first approximation, the mesomorphic state. However, we observed that there is not only a noninduction of mesomorphism but a disappearance of the monotropic mesophases N and S_A when X = OOC, and N when X = COO. This observation, in addition to the higher melting points of the complexes, leads us to the conclusion that the global effect of the introduction of the $[M(CO)_2]$ unit is a stabilization of the crystalline phase to the detriment of the mesomorphic phases.

Pyrazole Derivatives (7−9) (Table 2). Only complex **7** (X = COO) is mesomorphic and shows a monotropic nematic phase. The texture observed under the microscope is shown in Figure 1b (nematic drops with Schlieren texture). The pyrazole ligands HL'_1 and HL'_2 show monotropic nematic mesophases. Comparing these ligands with the complexes **7** and **8**, the addition of the $[RhCl(CO)_2]$ unit to the ligand structure maintains or even reduces the melting points. This behavior can be explained assuming that the metal unit restricts the interaction between the pyrazole rings through hydrogen bonds. As already mentioned for the β-diketonate metal derivatives, the introduction of the $[RhCl(CO)_2]$ unit in the pyrazole chain leads to a noninduction or worsening of the mesomorphic properties.

Single-Crystal X-ray Analysis of $[IrL_1(CO)_2]\cdot CH_3OH$ ($4\cdot CH_3OH$). An X-ray diffraction analysis of a tiny plate of the yellow polymorph of compound **4** was carried out. A molecular drawing of this molecule is shown in Figure 2. Selected bond distances and angles are listed in Table 3.

The β-diketonate ligand (L_1) is bonded in a chelate fashion to the metal center through the two oxygen atoms, O(3) and O(4); additionally, two carbonyl groups complete a slightly distorted square-planar environment at the iridium atom. The six-membered metallacycle formed is almost planar, with a maximum deviation from the mean plane of 0.026(8) Å for O(3). The Ir−O distances (2.038 and 2.027(7) Å) are very similar to those reported for the closely related compounds [M(acac)(cod)] (M = Ir, 2.039 and 2.045(3) Å,[12] or M = Rh, 2.040 and 2.044(4) Å [13]).

The whole molecule adopts an extended rodlike shape, with an all-trans conformation of the decyloxy chain. The orientation of ester group C1 (see Figure 2) with respect to the adjacent phenyl (B1) and metallacycle (acac) rings are described by the dihedral angles C1/B1 60.5(7)° and C1/acac 55.1(7)°, in such a way that these two rings are nearly parallel (9.9(3)°). In the case of the other carboxyl group, C2, the orientation with respect to the O- and C-bonded phenyl rings are 60.1 and 1.9(8)°. As expected, the relative orientations between carboxyl and phenyl groups are almost coplanar for the C-bonded and significantly rotated (60° approximately) for the O-bonded.[14] Interestingly, the principal molecular axis of the rodlike molecule is approximately parallel to the crystallographic *a* axis (Figure 3a). The packing arrangement in the *ac* plane situates contiguous molecules antiparallel, with adjacent molecules disposed in opposite senses. The solid-state molecular organization could be described as a layered structure (along the *bc* plane), each layer being formed by almost perpendicular molecules with alternate orientations. There exists some degree of interdigitation between two consecutive layers through the long hydrocarbonated chains (along the *a* axis approximately). As a result of this packing arrangement there is a stacking of the molecules along the short *b* axis (4.0093(8) Å), but with the metal coordination plane not perpendicular to this crystallographic axis (the angle

(11) Wan, W.; Guang, W.-J.; Zhao, K.-Q.; Zheng, W.-Z.; Zhang, L.-F. *J. Organomet. Chem.* **1998**, *557*, 157.
(12) Tucker, P. A. *Acta Crystallogr.* **1981**, *B37*, 1113.
(13) Huq, F.; Skapski, A. C. *J. Cryst. Mol. Struct.* **1974**, *4*, 411.
(14) Schweizer, W. B.; Dunitz, J. D. *Helv. Chim. Acta* **1982**, *65*, 1547.

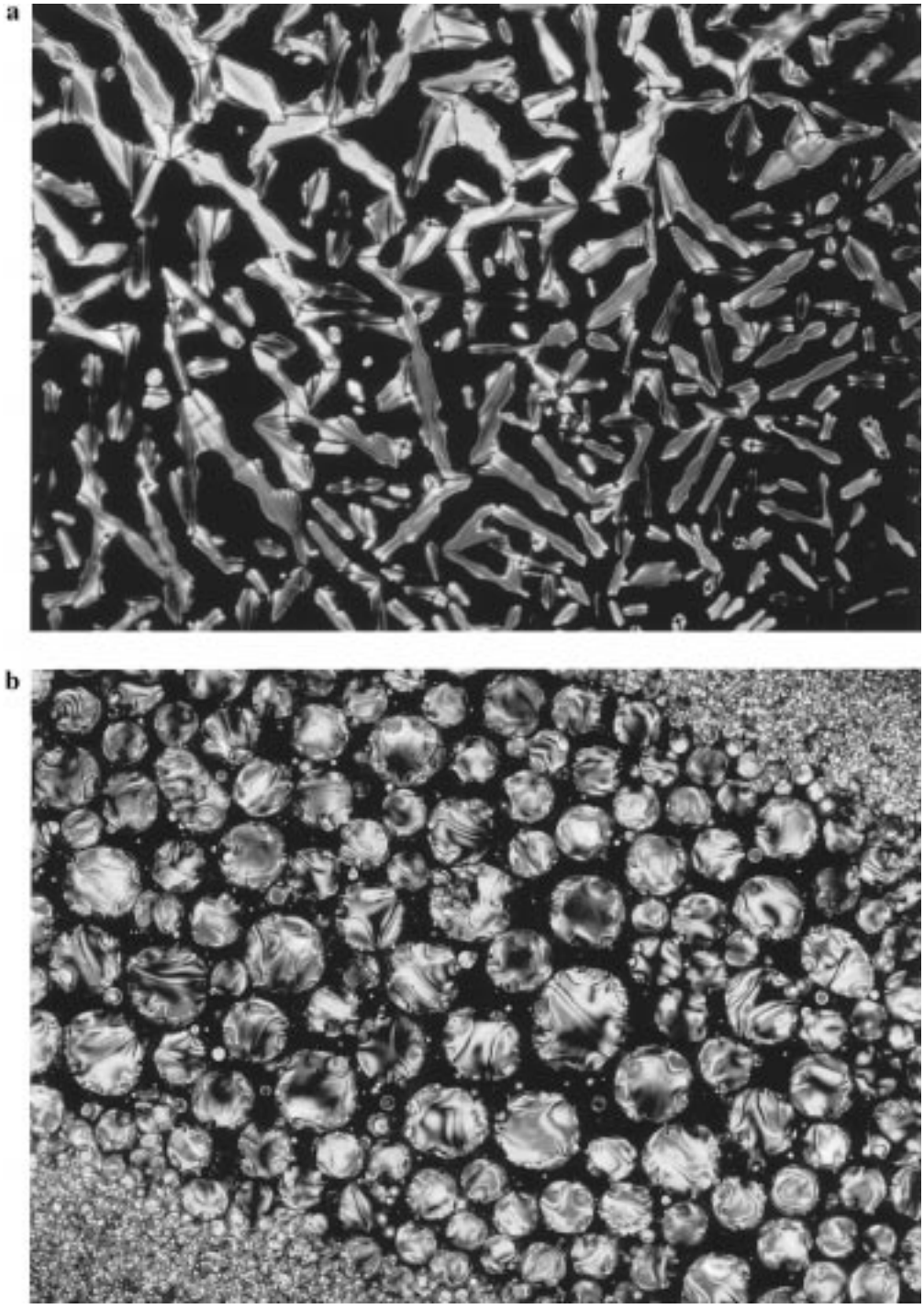

Figure 1. (a) Microphotograph of the texture of the smectic A mesophase of compound **1**. (b) Microphotograph of the texture of the nematic mesophase of compound **7**. Crossed polarizers.

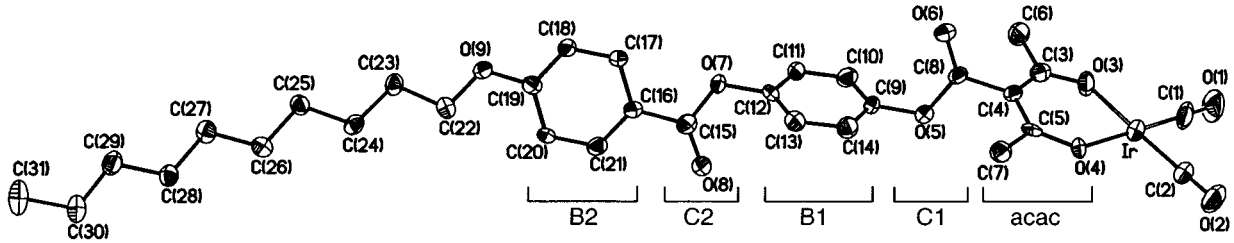

Figure 2. Molecular representation of **4** with numbering scheme used. An indication of the labeling used for calculated least-squares planes is also included.

between the *b* axis and the normal to the coordination plane is 24.5(2)°) (Figure 3b). This particular intermetallic disposition together with the long Ir···Ir separation seems to exclude a direct metal−metal interaction in this yellow polymorph.[9] However,

Table 3. Selected Bond Lengths (Å) and Angles (deg) for $[IrL_1(CO)_2]$ (**4**)[a]

Ir···Ir′	4.0093(12)		
Ir−C(1)	1.856(13)	Ir−C(2)	1.860(11)
Ir−O(3)	2.038(7)	Ir−O(4)	2.027(7)
O(1)−C(1)	1.130(15)	O(2)−C(2)	1.122(13)
O(3)−C(3)	1.293(12)	O(4)−C(5)	1.287(12)
C(3)−C(4)	1.389(15)	C(4)−C(5)	1.421(13)
O(5)−C(8)	1.368(13)	O(7)−C(15)	1.373(13)
O(5)−C(9)	1.426(11)	O(7)−C(12)	1.422(11)
O(6)−C(8)	1.192(12)	O(8)−C(15)	1.210(12)
C(1)−Ir−C(2)	88.6(5)	O(3)−Ir−O(4)	87.5(3)
C(1)−Ir−O(3)	91.4(4)	C(2)−Ir−O(4)	92.6(4)
C(1)−Ir−O(4)	178.2(5)	C(2)−Ir−O(3)	177.7(5)
Ir−C(1)−O(1)	178.5(11)	Ir−C(2)−O(2)	179.0(11)
Ir−O(3)−C(3)	128.1(7)	Ir−O(4)−C(5)	130.0(7)
O(3)−C(3)−C(4)	125.9(9)	O(4)−C(5)−C(4)	123.8(9)
C(3)−C(4)−C(5)	124.6(9)		

[a] Primed atom is related to the unprimed one by the symmetry transformation x, $1 + y$, z.

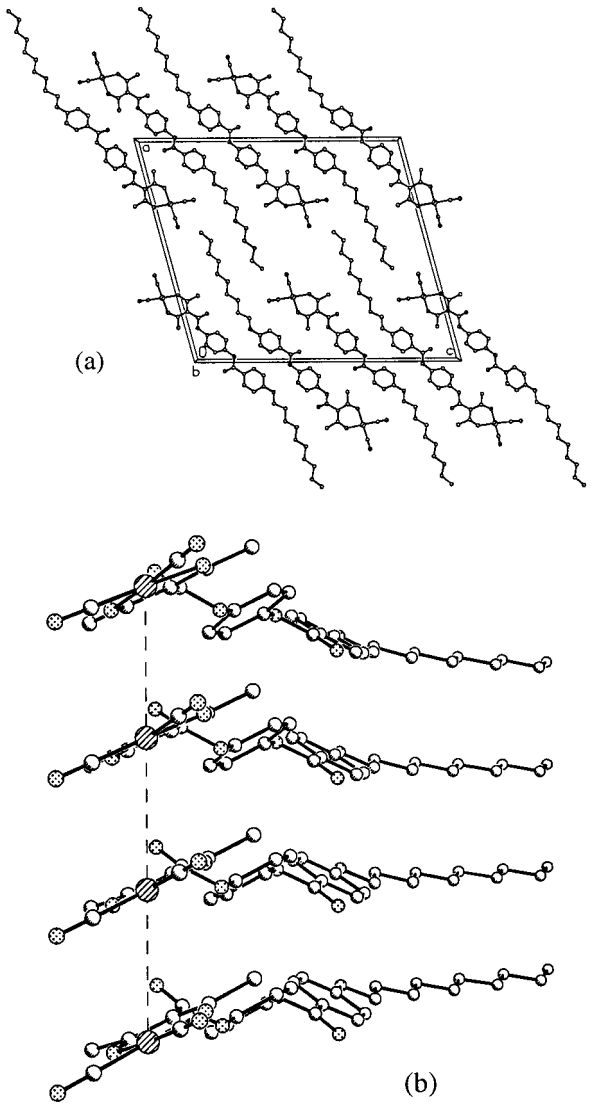

Figure 3. Drawing of the packing of molecules in **4**: (a) in the *ac* plane and (b) along the *b* axis.

it seems reasonable that under thermal stress a minor reorganization of the crystal could take place by a small rotation of the metal coordination planes to make them perpendicular to the crystallographic *b* axis. This situation will bring the d_{z^2} orbitals of the metal centers into alignment, and most likely the intermetallic interaction proposed for the high-temperature polymorph could take place generating a darker color for this alternative crystalline form.

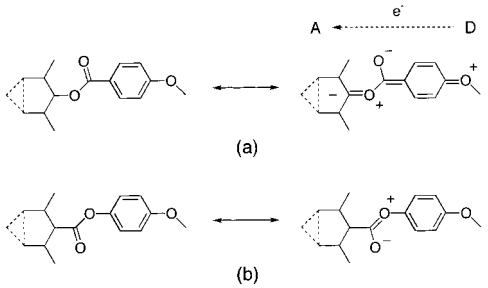

Figure 4. Charge transfer for molecules with X = OOC (a) and for molecules with X = COO (b). A is the acceptor group, and D is the donor group.

Table 4. Experimental $\mu_0\beta$ Values Measured at 1380 nm and $\mu_0\beta_0$ Values Deduced from a Two-Level Model (10^{-48} Esu) and Absorption Bands Maxima (nm) of β-Diketone and Pyrazole Derivatives

compd	X	λ_{max}	$(\mu_0\beta)_{1,38}$	$(\mu_0\beta_0)$
HL_1	COO	267	32	26
1	COO	268, 328	≈20	≈15
2	OOC	270, 323	46	34
3	CH_2	323	≈20	≈15
HL'_1	COO	263	18	15
HL'_2	OOC	274	31	25
7	COO	265, 339	26	18
8	OOC	270, 337	53	38
9	CH_2	265, 338	23	16

Nonlinear Optical Properties. The experimental $\mu_0\beta$ and the $\mu_0\beta_0$ values deduced from a simple two-level model[15] are shown in Table 4.

If we compare the ligands HL_1 and HL'_1, the higher $\mu_0\beta$ value of the former qualitatively agrees with the results obtained in other β-diketone and pyrazole derivatives.[16] The origin of this difference can be found in the stronger acceptor character of the β-diketone group as compared with the pyrazole.

The $\mu_0\beta$ values seem to reflect the global charge transfer in the whole molecule which can be modified in different ways by the local charge transfer in the COO and OOC ester groups. In the molecule as a whole, the charge moves from the *n*-decyloxy group to the β-diketone or pyrazole group, the same direction as in the X = OOC group, because the oxygen atom placed in the molecular axis is a π donor and could give charge to the main acceptor (Figure 4a). On the other hand, for X = COO, the π acceptor carbon atom of the ester group is directly linked to the main acceptor group and the charge transfer is partially interrupted. (Figure 4b). The relatively low $\mu_0\beta$ values of complexes **3** and **9** can also be explained in terms of charge transfer, as the CH_2 group disrupts the molecular conjugation.

The absorption spectra of rhodium−pyrazole complexes show a main band centered around 265−270 nm similar to that of the corresponding ligand (see Table 4). This band is assigned to a $\pi \rightarrow \pi^*$ intraligand transition. It also shows one smaller band at higher wavelength (around 338 nm) associated with a transition involving metal orbitals. As can be seen in Table 4, the rhodium−pyrazole complexes show slightly higher $\mu_0\beta$ values than their ligands. A similar behavior, with a more

(15) Oudar, J. L.; Chemla, D. S. *J. Chem. Phys.* **1977**, *66*, 2664.
(16) Barberá, J.; Giménez, R.; Serrano, J. L.; Alcalá, R.; Villacampa, B.; Villalba, J.; Ledoux, I.; Zyss, J. *Liq. Cryst.* **1997**, *22*, 265.
(17) Bruce, D. W.; Thornton, A. *Mol. Cryst. Liq. Cryst.* **1993**, *231*, 253.

Table 5. Crystallographic Data for $[IrL_1(CO)_2]\cdot CH_3OH$ (**4**·CH_3OH)

chem formula	$C_{32}H_{39}IrO_{10}$	ρ(calcd), g cm^{-3}	1.581
cryst color and habit	yellow, prismatic block	μ, mm^{-1}	4.151
fw	775.83	θ range data collecn, deg	2.3−25.0
temp, K	173(2)	index ranges	$-1 \le h \le +30$, $-1 \le k \le +4$, $-37 \le l \le +36$
cryst syst	monoclinic	collecd reflcns	7831
space group	$P2_1/c$ (No. 14)	unique reflcns	5625 ($R_{int} = 0.0629$)
a, Å	26.991(6)	abs corr method	ψ-scan
b, Å	4.0093(8)	min, max transm factors	0.273, 0.422
c, Å	31.169(6)	data/restraints/params	5625/107/394
β, deg	104.950(13)	$R(F)$ [$F^2 > 2\sigma(F^2)$][a]	0.0583
V, Å^3	3258.8(12)	$R_w(F^2)$ [all data][b]	0.1566
Z	4	S [all data][c]	1.040

[a] $R(F) = \sum||F_o| - |F_c||/\sum|F_o|$, for 3794 observed reflections. [b] $R_w(F^2) = (\sum[w(F_o^2 - F_c^2)^2]/\sum[w(F_o^2)^2])^{1/2}$. [c] $S = [\sum[w(F_o^2 - F_c^2)^2]/(n - p)]^{1/2}$; n = number of reflections, p = number of parameters.

important enhancement of the nonlinear response, has been previously observed in stilbazole derivative rhodium complexes.[11] The reported $\mu_0\beta$ value of the [RhCl(CO)$_2$(4-stilbazole)] complex is 149×10^{-48} esu bigger than that of the ligand (60×10^{-48} esu). Kanis et al.[18] explain similar results in other stilbazole complexes as resulting from the increase of the electron acceptor character of the pyridine cycle induced by the metal group. This also could explain the effect of the metal group [RhCl(CO)$_2$] in the pyrazole ligand.

The experimental $\mu_0\beta$ values obtained for the β-diketone ligand HL_1 and its complex show that the presence of the metal decreases the nonlinear response. To explain the difference between pyrazole and β-diketone derivatives, it is necessary to note that the metal environment is different in the two series of compounds ([RhCl(CO)$_2$] and [Rh(CO)$_2$], respectively), and the presence of a chlorine atom in the pyrazole complexes, acting as a charge acceptor, could be related to the enhancement of the nonlinear response.

Conclusions

New liquid crystal pyrazole or β-diketonate−rhodium or −iridium derivatives have been prepared. Two different polymorphs, for some of the β-diketonate compounds, have been obtained at the solid state. The color, as well as the infrared spectra displayed for the solids forms, seems to be related to a different intermetallic-packing arrangement suggesting a d_{z^2} orbital interaction for the metal centers in the dark solid polymorphs, as indicated by the X-ray crystallographic study made for compound **4**.

On the other hand, the presence of the metal in the rhodium−pyrazole derivatives leads to an enhancement of the nonlinear response, probably due to the presence of a chlorine atom bonded to the metal center acting as a charge acceptor. However, the β-diketonate derivatives, presenting a different metal environment, show the opposite trend.

Experimental Section

All reactions were carried out under argon using standard Schlenk techniques. The β-diketone ligands[1c] (HL_1, 3-[(4′-((4″-*n*-decyloxybenzoyl)oxy)phenoxy)carbonyl]-2,4-pentanedione; HL_2, 3-[(4′-((4″-*n*-decyloxybenzoyl)oxy)benzoyl)oxy]-2,4-pentanedione; HL_3, 3-[(4′-(4″-*n*-decyloxybenzoyl)oxy)benzyl]-2,4-pentanedione), the pyrazole ligands[1c]; (HL'_1, 4-[(4′-((4″-*n*-decyloxybenzoyl)oxy)phenoxy)carbonyl]-3,5-dimethylpyrazole; HL'_2, 4-[(4′-((4″-*n*-decyloxybenzoyl)oxy)benzoyl)oxy]-3,5-dimethylpyrazole; HL'_3, 4-[4′-((4″-*n*-decyloxybenzoyl)oxy)benzyl]-3,5-dimethylpyrazole)), $[Rh_2(\mu\text{-Cl})_2(COD)_2]$,[19] $[Rh_2(\mu\text{-Cl})_2(CO)_4]$,[20] and $[Ir_2(\mu\text{-Cl})_2(COD)_2]$[21] were prepared according to literature methods. Solvents were purified by standard procedures and distilled under argon prior to use. All other reagents were purchased from Aldrich and used as received.

Experimental Measurements. Infrared spectra, ^{1}H and ^{13}C NMR spectra, elemental analyses, optical textures of the mesophases, differential scanning calorimetries, absorption spectra, and EFISH measurements were recorded as previously described.[2d,8,16]

X-ray Structural Analysis of $[IrL_1(CO)_2]\cdot CH_3OH$ (4·CH_3OH). A summary of crystal data and refinement parameters is given in Table 5. Yellow crystals of **4** were obtained by slow diffusion of methanol in a concentrated solution of **4** in dichloromethane. A yellow plate of approximate dimensions $0.09 \times 0.25 \times 0.30$ mm was selected and used for data collection; diffraction data were measured with a Siemens P4 diffractometer using graphite-monochromated Mo K_α radiation ($\lambda = 0.710\ 73$ Å). Cell constants were obtained from the least-squares fit on the setting angles of 60 reflections in the range $20 \le 2\theta \le 35°$. A set of 7831 reflections with 2θ in the range 4−50° was measured using the ω scan technique and corrected for Lorentz and polarization effects; a semiempirical absorption correction, based on azimuthal ψ-scans from 20 reflections, was also applied.[22] Three standard reflections were measured every 97 reflections as a check of crystal and instrument stability; no important variation was observed.

The structure was solved by direct methods (SIR92)[23] and difference Fourier techniques and refined by full-matrix least squares on F^2 (SHELXL97),[24] first with isotropic and then with anisotropic displacement parameters for all non-hydrogen atoms. The hydrogen atoms were introduced in calculated positions and refined riding on the corresponding carbon atoms. At this stage, a difference Fourier map showed a heavily disordered solvent with peaks up to 2.61 e Å^{-3}. The Squeeze procedure[25] implemented in PLATON[26] was used to calculate the potential solvent volume (332.5 Å^3/unit cell) and the electron count missing in the model (64 e$^-$/unit cell approximately). With these data we decided to include one methanol solvent molecule per asymmetric unit (4×18 e$^-$) modeled as two carbon atoms disordered in five positions. The largest peak remaining in this solvent zone was 1.28 e Å^{-3}. The refinement converged at $R_w(F^2) = 0.1566$ for 394 parameters, 107 restraints, and 5625 unique reflections. The calculated weighting scheme is $1/[\sigma^2(F_o^2) + (0.0732P)^2 + 14.15P]$, where $P = (\max(F_o^2,0) + 2F_c^2)/3$. Scattering factors were used as implemented in the refinement program.[24] The largest peak and hole in the final difference map were 1.67 (close to iridium atom) and −0.97 e Å^{-3}.

Synthesis of the Complexes $[RhL(CO)_2]$ (L = L_1 (1), L_2 (2), L_3 (3). These compounds were prepared by two general methods:

(18) Kanis, D. R.; Lacroix, P. G.; Ratner, M. A. *J. Am. Chem. Soc.* **1994**, *116*, 10089.
(19) Giordano, G.; Crabtree, R. H. *Inorg. Synth.* **1979**, *19*, 218.
(20) Hieber, W.; Lagally, H. *Z. Anorg. Allg. Chem.* **1943**, *251*, 96.
(21) Herde, J. L.; Lambert, J. C.; Seneff, C. V. *Inorg. Synth.* **1974**, *15*, 18.
(22) North, A. C. T.; Phillips, D. C.; Mathews, F. S. *Acta Crystallogr.* **1968**, *A24*, 351.
(23) Altomare, A.; Cascarano, G.; Giacovazzo, C.; Guagliardi, A. *J. Appl. Crystallogr.* **1994**, *27*, 435.
(24) Sheldrick, G. M. *SHELXL-97*; University of Göttingen: Göttingen, Germany, 1997.
(25) Van der Sluis, P.; Spek, A. L. *Acta Crystallogr.* **1990**, *A46*, 194.
(26) Spek, A. L. *Acta Crystallogr.* **1990**, *A46*, C34.

Chart 1

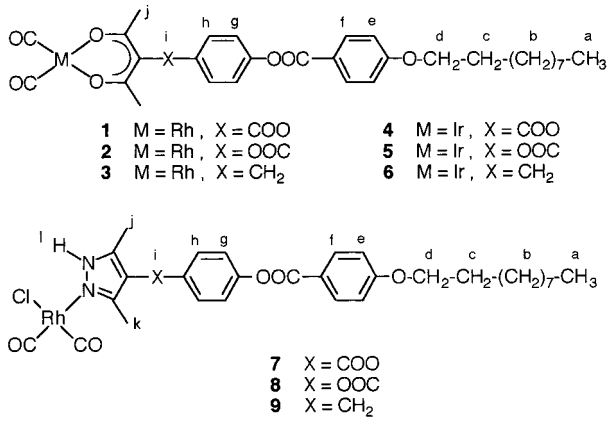

(a) Method 1. To a suspension of sodium diketonate (prepared in situ by reaction of β-diketone (HL_1−HL_3) (0.536 mmol) and sodium acetate (44 mg, 0.536 mmol), in methanol (15 mL), $[Rh_2(\mu\text{-}Cl)_2(CO)_4]$ (104 mg, 0.268 mmol) was added. The reaction mixture was stirred at room temperature for 1 h. Then, the resulting precipitate was separated by filtration, washed with methanol, and vacuum-dried.

(b) Method 2. Carbon monoxide was bubbled through a solution of [Rh(L)(COD)] (0.506 mmol) [prepared by reaction of potassium diketonate (KOH in methanol/β-diketone: 1.7 mL, 0.294 M/0.506 mmol) and $[Rh_2(\mu\text{-}Cl)_2(COD)_2]$ (124 mg, 0.252 mmol)] in diethyl ether (15 mL) for 30 min. The concentration of the solvent to 2 mL and addition of methanol (10 mL) afforded a solid which was separated by filtration and dried in a vacuum.

$[Rh(L_1)(CO)_2]$ (1). Compound **1** (see Chart 1) was isolated as two crystalline forms, red and yellow. The red form was obtained by precipitating the solid by evaporation of the solvent at high temperatures. The yellow form was precipitated at room temperature. Yield: 78−82% (method 1). IR (Nujol, NaCl, cm^{-1}). Red solid: 2081, 2027, 2005, 1978 (C≡O), 1742, 1731 (C═O), 1605 (ar C−C), 1580 (C═O), 1508 (ar C−C), 1254 (C−O). Yellow solid: 2088, 2027 (C≡O), 1735 (C═O), 1607 (ar C−C), 1586 (C═O), 1504 (ar C−C), 1254 (C−O). IR (CH_2Cl_2): 2089, 2017 (C≡O). ^1H NMR ($CDCl_3$): δ 0.87 (t, J = 6.6 Hz, 3H, H_a), 1.26−1.46 (m, 14H, H_b), 1.78−1.83 (m, 2H, H_c), 2.35 (s, 6H, H_j), 4.02 (t, J = 6.4 Hz, 2H, H_d), 6.95 (d, J = 8.8 Hz, 2H, H_e), 7.18 (d, J = 9.0 Hz, 2H, H_g) 7.24 (d, J = 9.0 Hz, 2H, H_f), 8.11 (d, J = 8.8 Hz, 2H, H_h). ^{13}C NMR ($CDCl_3$): δ 14.1, 22.6, 25.9, 27.5, 29.0, 29.3, 29.3, 29.5, 31.8, 68.3, 111.4, 114.3, 121.2, 122.8, 132.3, 147.8, 148.5, 163.6, 164.8, 167.9, 183.0 (d, J_{RhC} = 73 Hz), 188.6 (b). Anal. Calcd for $C_{31}H_{35}O_9Rh$: C, 56.89; H, 5.39. Found: C, 56.86; H, 5.25.

$[Rh(L_2)(CO)_2]$ (2). Compound **2** was isolated as a yellow microcrystalline solid. Yield: 79% (method 1). IR (Nujol, NaCl, cm^{-1}): 2080, 2008 (C≡O), 1736 (C═O), 1604 (ar C−C), 1585 (C═O), 1510 (ar C−C), 1254 (C−O). IR (CH_2Cl_2): 2080, 2010 (C≡O). ^1H NMR ($CDCl_3$): δ 0.87 (t, J = 6.7 Hz, 3H, H_a), 1.26−1.48 (m, 14H, H_b), 1.79−1.83 (m, 2H, H_c), 2.10 (s, 6H, H_j), 4.03 (t, J = 6.5 Hz, 2H, H_d), 6.97 (d, J = 8.9 Hz, 2H, H_e), 7.34 (d, J = 8.8 Hz, 2H, H_g) 8.13 (d, J = 8.9 Hz, 2H, H_f), 8.23 (d, J = 8.8 Hz, 2H, H_h). ^{13}C NMR ($CDCl_3$): δ 182.4 (b), 183.4 (d, J_{RhC} = 73 Hz). Anal. Calcd for $C_{31}H_{35}O_9Rh$: C, 56.89; H, 5.39. Found: C, 56.92; H, 5.18.

$[Rh(L_3)(CO)_2]$ (3). Compound **3** was isolated as a red solid. Yield: 85% (method 1). IR (Nujol, NaCl, cm^{-1}). Red solid: 2068, 1999, 1988 (C≡O), 1744, 1735 (C═O), 1605 (ar C−C), 1573 (C═O), 1511 (ar C−C), 1254 (C−O). IR (CH_2Cl_2): 2080, 2010 (C≡O). ^1H NMR ($CDCl_3$): δ 0.84 (t, J = 6.7 Hz, 3H, H_a), 1.26−1.45 (m, 14H, H_b), 1.77−1.82 (m, 2H, H_c), 2.10 (s, 6H, H_j), 3.73 (s, 2H, H_i), 4.02 (t, J = 6.5 Hz, 2H, H_d), 6.94 (d, J = 8.7 Hz, 2H, H_e), 7.10 (s, 4H, H_g, H_h), 8.10 (d, J = 8.7 Hz, 2H, H_f). ^{13}C NMR ($CDCl_3$): δ 183.9 (d, J_{RhC} = 73 Hz), 187.4 (b). Anal. Calcd for $C_{31}H_{37}O_7Rh$: C, 59.62; H, 5.97. Found: C, 59.58; H, 5.76.

Synthesis of the Complexes $[IrL(CO)_2]$ (L = L_1 (4), L_2 (5), L_3 (6). Complexes **4**−**6** were prepared by method 2 described for complexes **1**−**3** starting from β-diketone (0.236 mmol), KOH in methanol (0.8 mL, 0.294 M), and $[Ir_2(\mu\text{-}Cl)_2(COD)_2]$ (79.2 mg, 0.118 mmol).

$[Ir(L_1)(CO)_2]$ (4). Compound **4** was isolated as two crystalline forms, dark blue and yellow. The blue form was obtained by precipitating the solid by evaporation of the solvent at high temperatures. The yellow form was precipitated at room temperature. Yield: 68−72%. IR (Nujol, NaCl, cm^{-1}): Blue solid: 2067, 2022(b), 1983 (C≡O), 1731 (b) (C═O), 1605 (ar C−C), 1574 (C═O), 1510 (ar C−C), 1258 (C−O). Yellow solid: 2079, 1997 (C≡O), 1728 (C═O), 1607 (ar C−C), 1574 (C═O), 1511,1505 (ar C−C), 1259 (C−O). IR (CH_2Cl_2): 2077, 2000 (C≡O). ^1H NMR ($CDCl_3$): δ 0.87 (t, J = 6.5 Hz, 3H, H_a), 1.19−1.46 (m, 14H, H_b), 1.78−1.83 (m, 2H, H_c), 2.39 (s, 6H, H_j), 4.03 (t, J = 6.4 Hz, 2H, H_d), 6.96 (d, J = 8.8 Hz, 2H, H_e), 7.19 (d, J = 9.0 Hz, 2H, H_g), 7.25 (d, J = 9.0 Hz, 2H, H_f), 8.12 (d, J = 8.8 Hz, 2H, H_h). ^{13}C NMR ($CDCl_3$): δ 187.7. Anal. Calcd for $C_{31}H_{35}IrO_9$: C, 50.06; H, 4.74. Found: C, 50.12; H, 4.94.

$[Ir(L_2)(CO)_2]$ (5). Compound **5** was isolated as a yellow microcrystalline solid. Yield: 72%. IR (Nujol, NaCl, cm^{-1}): 2067, 1988 (C≡O), 1737 (C═O), 1603 (ar C−C), 1577 (C═O), 1510 (ar C−C), 1259 (C−O). IR (CH_2Cl_2): 2070, 1995 (C≡O). ^1H NMR ($CDCl_3$): δ 0.87 (t, J = 6.7 Hz, 3H, H_a), 1.26−1.46 (m, 14H, H_b), 1.78−1.81 (m, 2H, H_c), 2.11 (s, 6H, H_j), 4.03 (t, J = 6.5 Hz, 2H, H_d), 6.97 (d, J = 8.9 Hz, 2H, H_e), 7.36 (d, J = 8.7 Hz, 2H, H_g) 8.13 (d, J = 8.9 Hz, 2H, H_f), 8.24 (d, J = 8.7 Hz, 2H, H_h). ^{13}C NMR ($CDCl_3$): δ 182.0. Anal. Calcd for $C_{31}H_{35}IrO_9$: C, 50.06; H, 4.74. Found: C, 49.98; H, 4.53.

$[Ir(L_3)(CO)_2]$ (6). Compound **6** was isolated as two crystalline forms, dark blue and yellow. The blue form was obtained by precipitating the solid by evaporation of the solvent at high temperatures. The yellow form was precipitated at room temperature. Yield: 70−75%. IR (Nujol, NaCl, cm^{-1}). Blue solid: 2054, 2006(b), 1979, 1970 (C≡O), 1733 (C═O), 1605 (ar C−C), 1564 (C═O), 1510 (ar C−C), 1255 (C−O). Yellow solid: 2044, 1988, 1977 (C≡O), 1736, 1725 (C═O), 1603 (ar C−C), 1559 (C═O), 1509 (ar C−C), 1259 (C−O). IR (CH_2Cl_2): 2060, 1990 (C≡O). ^1H NMR ($CDCl_3$): δ 0.84 (t, J = 6.3 Hz, 3H, H_a), 1.26−1.48 (m, 14H, H_b), 1.77−1.82 (m, 2H, H_c), 2.14 (s, 6H, H_j), 3.79 (s, 2H, H_i), 4.02 (t, J = 6.5 Hz, 2H, H_d), 6.94 (d, J = 8.9 Hz, 2H, H_e), 7.11 (s, 4H, H_g, H_h), 8.11 (d, J = 8.9 Hz, 2H, H_f). ^{13}C NMR ($CDCl_3$): δ 186.6. Anal. Calcd for $C_{31}H_{37}IrO_7$: C, 52.16; H, 5.22. Found: C, 52.02; H, 5.51.

Synthesis of the Complexes *cis*-$[RhCl(CO)_2(HL')]$ (L′ = L'_1 (7), L'_2 (8), L'_3 (9)). The appropriate pyrazole ligand (0.305 mmol) was added to a solution of $[Rh_2(\mu\text{-}Cl)_2(CO)_4]$ (59.3 mg, 0.152 mmol) in dichloromethane (10 mL). The reaction mixture was stirred for 30 min, and the solvent was concentrated to 0.5 mL. Addition of hexane (5 mL) led to the precipitation of a solid which was separated by filtration and recrystallized from dichloromethane/hexane.

***cis*-$[RhCl(CO)_2(HL'_1)]$ (7).** Compound **7** was isolated as a yellow solid. Yield: 78%. IR (Nujol, NaCl, cm^{-1}): 2086, 2078, 2020, 2009 (C≡O), 1731 (C═O), 1605, 1505 (ar C−C), 1258 (C−O). IR (CH_2Cl_2): 2100, 2020 (C≡O). ^1H NMR ($CDCl_3$): δ 0.86 (t, J = 6.8 Hz, 3H, H_a), 1.20−1.52 (m, 14H, H_b), 1.77−1.81 (m, 2H, H_c), 2.60 (s, 6H, H_j), 2.72 (s, 3H, H_k) 4.03 (t, J = 6.6 Hz, 2H, H_d), 6.95 (d, J = 8.8 Hz, 2H, H_e), 7.18−7.27 (m, 4H, H_f, H_g) 8.12 (d, J = 8.8 Hz, 2H, H_h), 11.57 (b, 1H, H_l). ^{13}C NMR ($CDCl_3$): δ 12.9, 14.2, 15.8, 22.6, 25.9, 29.0, 29.3, 29.3, 29.5, 31.9, 68.3, 110.3, 114.3, 121.2, 122.5, 122.8, 132.3, 147.2, 147.8, 148.7, 155.3, 161.0, 163.6, 164.8, 180.0 (b). Anal. Calcd for $C_{31}H_{36}N_2ClO_7Rh$: C, 54.20; H, 5.28; N, 4.08. Found: C, 53.80; H, 5.21; N, 4.09.

***cis*-$[RhCl(CO)_2(HL'_2)]$ (8).** Compound **8** was isolated as a yellow solid. Yield: 80%. IR (Nujol, NaCl, cm^{-1}): 2096, 2022 (C≡O), 1731 (C═O), 1604, 1510 (ar C−C), 1264 (C−O). IR (CH_2Cl_2): 2100, 2020 (C≡O). ^1H NMR ($CDCl_3$): δ 0.87 (t, J = 6.6, 3H, H_a), 1.26−1.52 (m, 14H, H_b), 1.77−1.82 (m, 2H, H_c), 2.23 (s, 6H, H_j), 2.31 (s, 3H, H_k) 4.04 (t, J = 6.6, 2H, H_d), 6.97 (d, J = 8.8, 2H, H_e), 7.37(d, J = 8.8, 2H, H_g), 8.13 (d, J = 8.8, 2H, H_f), 8.24 (d, J = 8.8, 2H, H_h), 11.30 (b, 1H, H_l). ^{13}C NMR ($CDCl_3$): δ 180.0 (b). Anal. Calcd for $C_{31}H_{36}N_2ClO_7Rh$: C, 54.20; H, 5.28; N, 4.08. Found: C, 54.17; H, 5.22; N, 3.98.

***cis*-$[RhCl(CO)_2(HL'_3)]$ (9).** Compound **9** was isolated as a yellow solid. Yield: 75%. IR (Nujol, NaCl, cm^{-1}): 2069, 2009 (C≡O), 1736

(C═O), 1606, 1511 (ar C−C), 1251 (C−O). IR (CH_2Cl_2): 2080, 2010 (C≡O). ^{1}H NMR ($CDCl_3$): δ 0.86 (t, J = 6.8 Hz, 3H, H_a), 1.26−1.52 (m, 14H, H_b), 1.77−1.82 (m, 2H, H_c), 2.19 (s, 6H, H_j), 2.29 (s, 3H, H_k) 3.75(s, 2H, H_i), 4.02 (t, J = 6.6 Hz, 2H, H_d), 6.94 (d, J = 8.8 Hz, 2H, H_e), 7.09 (s, 4H, H_g, H_h), 8.10 (d, J = 8.8 Hz, 2H, H_f), 11.09 (b, 1H, H_l). ^{13}C NMR ($CDCl_3$): δ 180.2(d, J_{RhC} = 62 Hz), 183.1(d, J_{RhC} = 62 Hz). Anal. Calcd for $C_{31}H_{38}N_2ClO_5Rh$: C, 56.67; H, 5.83; N, 4.26. Found: C, 56.68; H, 5.91; N, 4.27.

Acknowledgment. We thank the DGICYT (Project PB94-1186; Programa De Promoción General Del Conocimiento) and CICYT (Project MAT96-1073) for Financial Support and the Diputación General De Aragón for a Research Studentship to R. G.

Supporting Information Available: Crystallographic data, fractional atomic coordinates, anisotropic displacement parameters, hydrogen coordinates, bond distances and angles, and some least-squares planes, in CIF format. This material is available free of charge via the Internet at http://pubs.acs.org.

IC9814017